JOURNAL OF SOLID STATE CHEMISTRY 120, 204–207 (1995)

LETTER TO THE EDITOR

Effect of the Internal Pressure Due to the A-Site Cations on the Giant Magnetoresistance and Related Properties of Doped Rare Earth Manganates, $Ln_{1-x}A_xMnO_3$ (Ln = La, Nd, Gd, Y; A = Ca, Sr, Ba, Pb)

R. Mahesh,* R. Mahendiran,† A. K. Raychaudhuri,† and C. N. R. Rao*,[1]

*Solid State and Structural Chemistry Unit and †Department of Physics, Indian Institute of Science, Bangalore 560012, India

Communicated by J. M. Honig, September 8, 1995; accepted September 13, 1995

Based on an extensive study of a large variety of rare earth manganates (rare earth = La, Nd, Gd, or Y) with Ca, Sr, Ba, and Pb as the substituents, as well as of $LaMnO_3$ samples with varying Mn^{4+} content, it is shown that the ferromagnetic transition temperature, T_c, as well as the insulator–metal (I–M) transition temperature, T_p, increases with the weighted average radius of the A-cations, $\langle r_A \rangle$, showing a maximum at 1.23 ± 0.01 Å. The essentially linear region ($\langle r_A \rangle$ = 1.18–1.24 Å) demarcates the ferromagnetic metal and paramagnetic insulator regimes. The peak resistivity at the I–M transition, as well as the magnitude of the magnetoresistance (MR), decreases with increasing $\langle r_A \rangle$. Only below a $\langle r_A \rangle$ of 1.23 ± 0.01 Å is the MR greater than 50%.

The phenomenon of giant magnetoresistance (GMR) in oxides of the type $Ln_{1-x}A_xMnO_3$ (Ln = rare earth; A = divalent ion) has been the subject of intense investigation in the last two years (1–7). All the manganates show an insulator–metal (I–M) transition with a peak in the electrical resistivity, ρ_P, at a temperature T_p close to the ferromagnetic transition temperature, T_c. A giant negative magnetoresistance is generally encountered in the region near T_c. The magnitude of the MR and of the related properties such as T_c are determined by the Mn^{4+} content, around 30% Mn^{4+} being optimal. Some studies reported very recently (8–11) indicate that the T_c of $Ln_{1-x}A_xMnO_3$ varies systematically with the ionic radius of the A-site cation. An increase in the average radius of the A-site cation appears to be equivalent to the application of hydrostatic pressure (10). We have investigated several series of rare earth manganates with a view to studying the effect of internal pressure due to the A-site cations on the MR and the associated properties such as T_c, T_p, and ρ_P. Besides a large number of $La_{1-x}A_xMnO_3$ (A = a divalent ion) derivatives including Pb substituted ones, we have investigated the $La_{0.5}Ca_{0.5-z}Y_zMnO_3$ series as well as the $Nd_{1-x}A_xMnO_3$ and $Gd_{1-x}A_xMnO_3$ (A = Ca, Sr, Ba) series, all prepared and characterized under standardized conditions. The parent $LaMnO_3$ compositions with varying Mn^{4+} content arising from the presence of A- and B-site vacancies (12) examined here constitute a unique GMR system without aliovalent ion substitution. More importantly, we have followed the variation of both the ferromagnetic transition temperature, T_c, obtained from magnetic measurements and the I–M transition temperature, T_p, obtained from resistivity measurements. We have also studied the changes in the peak resistivity, ρ_p, at the I–M transition, which is more relevant to the GMR phenomenon than the room temperature resistivity ($T > T_p$, T_c).

All the manganates of the general formula $Ln_{1-x}A_xMnO_3$ (Ln = La, Nd, Gd, or Y; A = Ca, Sr, Ba, or Pb), as well as the parent $LaMnO_3$ samples with different Mn^{4+} content, were prepared by the solid state reaction of the relevant metal oxides or/and carbonates around 1273 K. The manganates were characterized by X-ray diffraction and the Mn^{4+} content was determined by redox titrations. Electrical resistivity and magnetoresistance measurements were made on bar-shaped pellets by the 4-probe method in the 4.2–350 K range. Magnetic fields up to 6 T were employed. Ferromagnetic Curie temperatures were determined by employing ac susceptibility and magnetization measurements. The magnetoresistance (MR) is defined as $[\rho(H)-\rho(0)]/\rho(0)$, where $\rho(H)$ and $\rho(0)$ are the resistivities at magnetic field H and at zero field respectively.

To understand the effect of the rare earth on the MR and other properties of $Ln_{1-x}A_xMnO_3$, it is instructive to compare the behavior of the members of the Ln_{1-x}

[1] To whom correspondence should be addressed.

0022-4596/95 $12.00

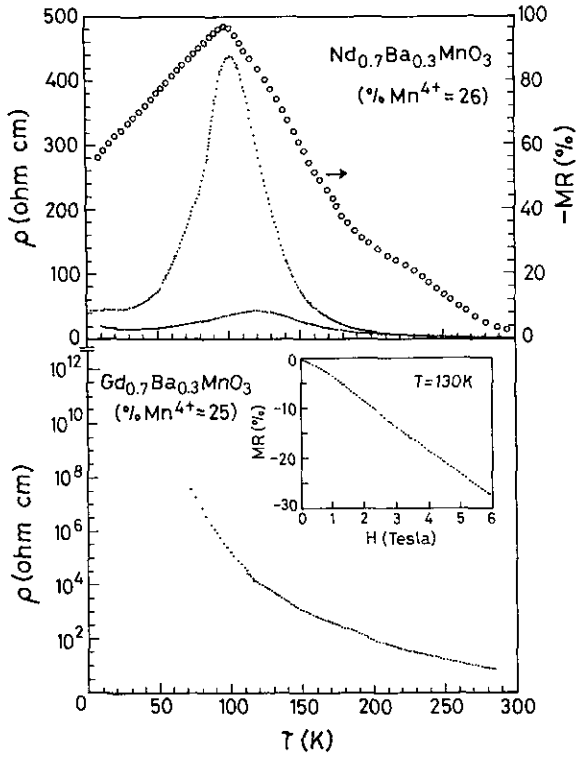

FIG. 1. (a) Temperature variation of the electrical resistivity (at 0 and 6 T) and of the percent magnetoresistance (%MR) of $Nd_{0.7}Ba_{0.3}MnO_3$. (b) Temperature variation of the electrical resistivity of $Gd_{0.7}Ba_{0.3}MnO_3$ at 0 T. Inset shows the variation of %MR with magnetic field at 130 K.

A_xMnO_3 series, where Ln = La, Nd, or Gd. In $Ln_{0.7}Ba_{0.3}MnO_3$, the T_p (T_c) decreases from 230 K (315 K) when Ln = La to 105 K (140 K) when Ln = Nd; $Gd_{0.7}Ba_{0.3}MnO_3$ is an insulator not showing a peak in resistivity. Similarly, in $Ln_{0.7}Sr_{0.3}MnO_3$, T_p (T_c) decreases from 330 K (360 K) when Ln = La to 185 K (195 K) when Ln = Nd; when Ln = Gd, the material is insulating. All these manganates are generally cubic with the Mn^{4+} content in the 25–37% range (Table 1). In $La_{0.5}Ca_{0.5-z}Y_zMnO_3$ compositions, which are also cubic, T_p decreases from 175 K when x = 0.05 to 85 K when x = 0.35. Clearly, a decrease in the size of the rare earth ion decreases T_p (T_c), due to the negative pressure effect of the smaller ion. In Fig. 1 we compare the magnetoresistance behavior of $Nd_{0.7}Ba_{0.3}MnO_3$ and $Gd_{0.7}Ba_{0.3}MnO_3$, both of which are cubic and have a Mn^{4+} content of ~25%. $Nd_{0.7}Ba_{0.3}MnO_3$ exhibits a sharp I–M transition and a fairly large GMR. $Gd_{0.7}Ba_{0.3}MnO_3$, on the other hand, shows no evidence for an I–M transition and hence no T_p. Accordingly, the observed MR is rather small, being 25% at 130 K (at 6 T). The field dependence of the MR of this composition is also unusual (Fig. 1b), in that we do not see the two distinct regimes evidenced in most of the manganates (6).

Results of our studies of several of the divalent ion-substituted rare earth manganates aptly demonstrate the effect of internal pressure induced by the A-site cations. In Fig. 2, we have plotted T_c and T_p values of $La_{1-x}A_xMnO_3$ (A = Ca, Sr, Ba, Pb) as well as of $La_{0.5}Ca_{0.5-z}Y_zMnO_3$ (most of which have the cubic structure) against the weighted average ionic radius of the A-site cation, $\langle r_A \rangle$, assuming ninefold coordination (13). T_p (T_c) increases with increased $\langle r_A \rangle$ and reaches a maximum around 1.23 ± 0.01 Å, above which T_p (T_c) decreases. Interestingly, T_p (T_c) values of parent $LaMnO_3$ with differing Mn^{4+} content also fall on the curve of $La_{1-x}A_xMnO_3$ systems. Since the manganates with $\langle r_A \rangle > 1.21$ Å studied by us are all cubic, we believe that the decrease in T_p (T_c) at high $\langle r_A \rangle$ may be due to the size mismatch between the cations. Such a size mismatch becomes even greater in $Nd_{1-x}Ba_xMnO_3$, which shows considerably different T_p (T_c) values from $La_{1-x}Ba_xMnO_3$. We note here that the data points for the A = Ca and Sr derivatives fall on the same curve in Fig. 2. We have shown the T_p (T_c) data for $Nd_{1-x}A_xMnO_3$ separately in the inset of Fig. 2; this curve has a shape similar to that exhibited by the large variety of other substituted manganates in Fig. 2, but the MR is anomalously high (Table 1). The curve in Fig. 2 is nearly linear in the $\langle r_A \rangle$ range of 1.18–1.24 Å and this region separates the ferromagnetic metal and the paramagnetic insulator regimes in the manganates.

In Fig. 3, we have plotted the maximum value of MR in the T_p (T_c) region against $\langle r_A \rangle$ for $Ln_{1-x}A_xMnO_3$ and

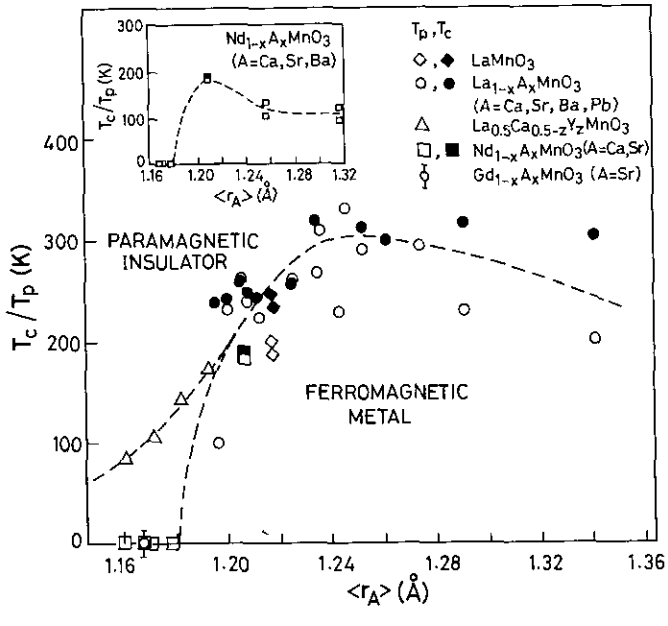

FIG. 2. Variation of T_p (T_c) of $Ln_{1-x}A_xMnO_3$ with the weighted average radius of the A-site cations, $\langle r_A \rangle$. In the inset, the data on $Nd_{1-x}A_xMnO_3$ are shown separately. The broken curve is drawn as a guide to the eye in this and subsequent figures.

TABLE 1
Properties of $Ln_{1-x}A_xMnO_3$ (Ln = La, Nd, or Gd; A = Sr or Ba)

Composition	% Mn^{4+}	Cubic a (Å)	T_p (K)	T_c (K)	ρ_P (ohm cm)	MR (%)
$La_{0.7}Ba_{0.3}MnO_3$	31	7.798	235	315	5	50
$Nd_{0.7}Ba_{0.3}MnO_3$	26	7.751	105	140	440	96
$Gd_{0.7}Ba_{0.3}MnO_3$	25	7.725	[a]	—	[a]	28[b]
$La_{0.5}Ba_{0.5}MnO_3$	45	7.781	200	300	3	48
$Nd_{0.5}Ba_{0.5}MnO_3$	43	7.743	95	120	210	92
$La_{0.7}Sr_{0.3}MnO_3$	37	[c]	330	360	0.02	45
$Nd_{0.7}Sr_{0.3}MnO_3$[d]	28	7.738	185	195	5	54

[a] Does not show a peak down to 50 K; $\rho = 10^4$ ohm cm at 130 K.
[b] Value at 130 K.
[c] Rhombohedral, $a = 5.454$ Å, $\alpha = 60.14°$.
[d] $Gd_{0.7}Sr_{0.3}MnO_3$ is an insulator down to 50 K.

$LaMnO_3$ compositions. We see that the MR decreases with increasing $\langle r_A \rangle$. In the inset of the same figure, we have plotted log ρ_P against $\langle r_A \rangle$ to demonstrate how the resistivity at the insulator–metal transition decreases with increased $\langle r_A \rangle$, just as the MR does. A high MR is generally associated with low T_p (T_c) and high ρ_P, both of which are favored by a smaller radius of the A-site cation.

A strict comparison of the MR and related properties of the manganate systems can be made only when the Mn^{4+} content is comparable. For this purpose, we have plotted the T_p (T_c) and %MR of manganates containing around 30% Mn^{4+} against $\langle r_A \rangle$ in Fig. 4. We see that the shape of the T_p (T_c) vs $\langle r_A \rangle$ curve is similar to that in Fig. 2, with a maximum around 1.23 ± 0.01 Å. The only difference is in the small $\langle r_A \rangle$ region where we had included T_c = 0 K data for some of the insulating manganates in Fig. 2. We generally do not observe T_c = 0 K in samples with ~30% Mn^{4+}; hence the difference. Figure 4b shows how the magnitude of MR smoothly decreases with increasing $\langle r_A \rangle$. In the inset of Fig. 4b, we have shown the variation of log ρ_P with $\langle r_A \rangle$ for the manganates with 30% Mn^{4+}; the variation is similar to that in Fig. 3.

Based on the present study, it seems necessary to make a judicious choice of A-site cations (with the right average

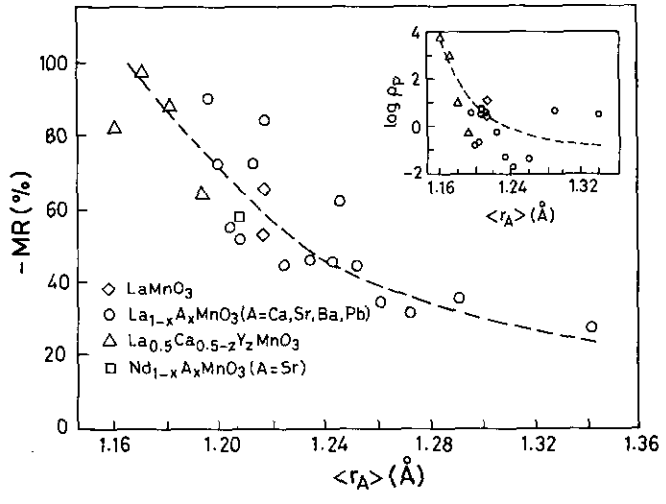

FIG. 3. Variation of the %MR with the weighted average ionic radius of the A-site cations, $\langle r_A \rangle$. The inset shows the variation of the logarithm of the resistivity at the I–M transition (log ρ_P) with $\langle r_A \rangle$.

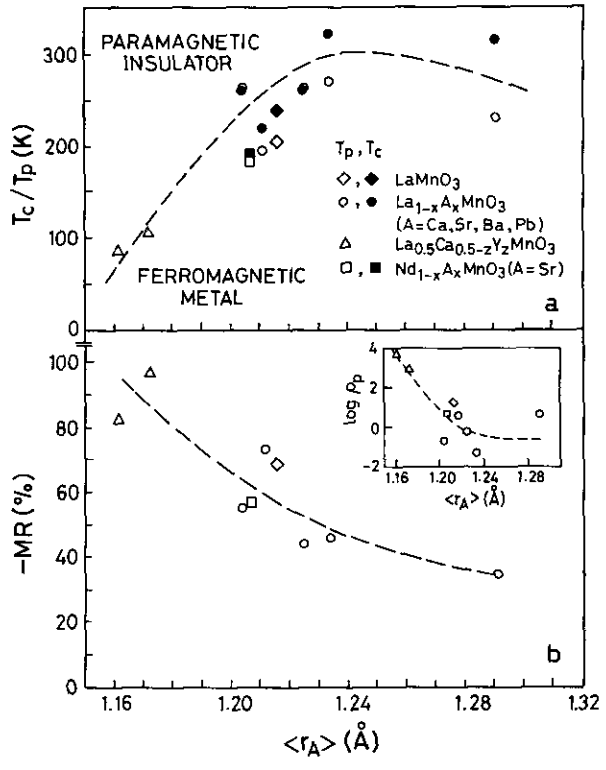

FIG. 4. (a) Variation of T_p (T_c) with $\langle r_A \rangle$ for manganates containing 30 ± 4% Mn^{4+}. (b) Variation of %MR with $\langle r_A \rangle$ for manganates containing 30 ± 4% Mn^{4+}. Inset shows the variation of log ρ_P with $\langle r_A \rangle$.

radius) in order to obtain the desired magnitudes of the various properties associated with the GMR phenomenon. When doing this, it should be noted that the T_p (T_c) maximum occurs close to a $\langle r_A \rangle$ of 1.23 ± 0.01 Å, which corresponds to a tolerance factor of 0.93. A high MR (>50%) is generally observed when $\langle r_A \rangle < 1.23$ Å. Typical of the manganates with $\langle r_A \rangle$ of 1.23 ± 0.01 Å are $La_{1-x}Sr_xMnO_3$ ($x = 0.1$–0.3) and cubic $LaMnO_3$.

ACKNOWLEDGMENTS

The authors thank the Department of Science and Technology for support. One of the authors (R.M.) thanks CSIR, India, for a fellowship.

REFERENCES

1. K. Chanara, T. Ohno, M. Kasai, and Y. Kozono, *Appl. Phys. Lett.* **63,** 1990 (1993).
2. R. von Helmolt, J. Wecker, B. Holzapfel, L. Schultz, and K. Samwer, *Phys. Rev. Lett.* **71,** 2331 (1993).
3. M. McCormack, S. Jin, T. Tiefel, R. M. Fleming, J. M. Phillips, and R. Ramesh, *Appl. Phys. Lett.* **64,** 3045 (1994).
4. A. Urushibara, Y. Moritomo, T. Arima, A. Asamitsu, G. Kido, and Y. Tokura, *Phys. Rev. B* **51,** 14,103 (1995).
5. H. L. Ju, J. Gopalakrishnan, J. L. Peng, Q. Li, G. C. Xiong, T. Venkatesan, and R. L. Greene, *Phys. Rev. B* **51,** 6143 (1995).
6. R. Mahesh, R. Mahendiran, A. K. Raychaudhuri, and C. N. R. Rao, *J. Solid State Chem.* **114,** 297 (1995); R. Mahendiran, R. Mahesh, A. K. Raychaudhuri, and C. N. R. Rao, *J. Phys. D Appl. Phys.* **28,** 1743 (1995); R. Mahendiran, R. Mahesh, N. Rangavittal, S. K. Tewari, A. K. Raychaudhuri, T. V. Ramakrishnan, and C. N. R. Rao, *Phys. Rev. B,* in press.
7. B. Raveau, A. Maignan, and V. Caignaert, *J. Solid State Chem.* **117,** 424 (1995).
8. Y. X. Jia, Li Lu, K. Khazeni, D. Yen, C. S. Lee, and A. Zettl, *Solid State Commun.* **94,** 917 (1995); V. Caignaert, A. Maignan, and B. Raveau, *Solid State Commun.* **95,** 357 (1995).
9. S. Jin, H. M. O'Bryan, T. H. Tiefel, M. McCormack, and W. W. Rhodes, *Appl. Phys. Lett.* **66,** 382 (1995).
10. H. Y. Hwang, S. W. Cheong, P. G. Radaelli, M. Marezio, and B. Batlogg, *Phys. Rev. Lett.* **75,** 914 (1995).
11. H. Y. Hwang, T. T. M. Palstra, S. W. Cheong, and B. Batlogg, preprint.
12. M. Verelst, N. Rangavittal, and C. N. R. Rao, *J. Solid State Chem.* **104,** 74 (1993); R. Mahesh, K. R. Kannan, and C. N. R. Rao, *J. Solid State Chem.* **114,** 294 (1995); M. Hervieu, R. Mahesh, N. Rangavittal and C. N. R. Rao, *Eur. J. Solid State Inorg. Chem.* **32,** 79 (1995).
13. S. Jin, M. McCormack, and T. H. Tiefel, *J. Appl. Phys.* **76,** 6929 (1994).